

**A DPF Analysis yields Full Analytic Potentials for
the $B^1\Pi_{1u}$ “Barrier” States of Rb_2 and Li_2 , *and*
An Improved Ground-State Well Depth and
Potential Energy Function for Rb_2**

Kai Slaughter,^a Nike Dattani,^b Claude Amiot,^c Amanda Ross,^d
and **Robert J. Le Roy**,^a

^a Department of Chemistry, University of Waterloo, Waterloo, Ontario, Canada.

^b Graduate School of Science, Department of Chemistry, Kyoto University, Kyoto, Japan.

^c Laboratoire Aimé Cotton, Bâtiment 505, Campus d'Orsay, 91405 Orsay CEDEX, France.

^d Institut de Lumière Matière, Université Claude Bernard Lyon 1, 69622 Villeurbanne
CEDEX, France.

Research supported by the Natural Sciences and Engineering Research Council of Canada.

Gaseous Atomic Rb has been of considerable interest in recent years

- as a medium for laser-cooling experiments
- as the material used for the first demonstration of Bose-Einstein condensation in a dilute medium
- as a medium for studying Feshbach resonances in ultra-cold atomic collisions

Gaseous Atomic Rb has been of considerable interest in recent years

- as a medium for laser-cooling experiments
- as the material used for the first demonstration of Bose-Einstein condensation in a dilute medium
- as a medium for studying Feshbach resonances in ultra-cold atomic collisions

Developing a proper understanding of such phenomena, and predicting related properties, such as binary collision parameters for ultracold mixed-isotope collisions and mixed isotope Bose–Einstein condensation, all depend upon having *an accurate knowledge of the potential energy functions* governing the behaviour of colliding Rb atoms.

However . . .

Ab initio calculations for this system are quite challenging . . .

- In 2001, Park *et al.*¹ reported new large-scale CI calculations using spin-averaged relativistic effective core potentials to determine an improved ground-state potential, but its well depth was 166 cm^{-1} too shallow.

¹S.J. Park, S.W. Suh, Y.S. Lee and G.-H. Jeung, *J. Mol. Spectrosc.* **207**, 129 (2001).

Ab initio calculations for this system are quite challenging . . .

- In 2001, Park *et al.*² reported new large-scale CI calculations using spin-averaged relativistic effective core potentials to determine an improved ground-state potential, but its well depth was 166 cm^{-1} too shallow.
- A 2006 paper³ setting out to obtain “... the best *a priori* predictions of the collisional properties of ground-state Rb atoms from the best available *ab initio* interatomic potentials” began by noting that the current most accurate theoretical potential functions dated back to the 1990 “effective core potentials” and “core polarization potentials (CPP)” of Krauss and Stevens,⁴ but its well was $\sim 50 \text{ cm}^{-1}$ too deep.

² S.J. Park, S.W. Suh, Y.S. Lee and G.-H. Jeung, *J. Mol. Spectrosc.* **207**, 129 (2001).

³ S Geltman, *J. Phys. B: At. Mol. Opt. Phys.* **39**, 4563 (2006).

⁴ M. Krauss and W.J. Stevens, *J. Chem. Phys.* **93**, 4236 (1990).

***Ab initio* calculations for this system are quite challenging . . .**

- In 2001, Park *et al.*⁵ reported new large-scale CI calculations using spin-averaged relativistic effective core potentials to determine an improved ground-state potential, but its well depth was 166 cm^{-1} too shallow.
- A 2006 paper⁶ setting out to obtain “... the best *a priori* predictions of the collisional properties of ground-state Rb atoms from the best available *ab initio* interatomic potentials” began by noting that the current most accurate theoretical potential functions dated back to the 1990 “effective core potentials” and “core polarization potentials (CPP)” of Krauss and Stevens,⁷ but its well was $\sim 50 \text{ cm}^{-1}$ too deep.

Empirical analyses for this state are in better shape, as . . .

- the most most recent 2000⁸ and 2010⁹ studies are in excellent agreement, yielding well-depth estimates, respectively, of $3993.53(\pm 0.06) \text{ cm}^{-1}$ and $3993.593(\pm 0.003) \text{ cm}^{-1}$ that agree to within their mutual uncertainties.

⁵ S.J. Park, S.W. Suh, Y.S. Lee and G.-H. Jeung, *J. Mol. Spectrosc.* **207**, 129 (2001).

⁶ S Geltman, *J. Phys. B: At. Mol. Opt. Phys.* **39**, 4563 (2006).

⁷ M. Krauss and W.J. Stevens, *J. Chem. Phys.* **93**, 4236 (1990).

⁸ J.Y. Seto, R.J. Le Roy, J. Vergès and C. Amiot, *J. Chem. Phys.* **113**, 3067 (2000)

⁹ C. Strauss, T. Takekoshi, F. Lang, K. Winkler, R. Grimm, J.H. Denschlag, and E. Tiemann, *Phys. Rev. A* **82**, 052514 (2010).

***Ab initio* calculations for this system are quite challenging . . .**

- In 2001, Park *et al.*¹⁰ reported new large-scale CI calculations using spin-averaged relativistic effective core potentials to determine an improved ground-state potential, but its well depth was 166 cm^{-1} too shallow.
- A 2006 paper¹¹ setting out to obtain “... the best *a priori* predictions of the collisional properties of ground-state Rb atoms from the best available *ab initio* interatomic potentials” began by noting that the current most accurate theoretical potential functions dated back to the 1990 “effective core potentials” and “core polarization potentials (CPP)” of Krauss and Stevens,¹² but its well was $\sim 50 \text{ cm}^{-1}$ too deep.

Empirical analyses for this state are in better shape, as . . .

- the most most recent 2000¹³ and 2010¹⁴ studies are in excellent agreement, yielding well depth estimates, respectively, of $3993.53(\pm 0.06) \text{ cm}^{-1}$ and $3993.593(\pm 0.003) \text{ cm}^{-1}$ that agree to within their mutual uncertainties.

However, information about most excited-state potentials is much thinner . . .

¹⁰ S.J. Park, S.W. Suh, Y.S. Lee and G.-H. Jeung, *J. Mol. Spectrosc.* **207**, 129 (2001).

¹¹ S Geltman, *J. Phys. B: At. Mol. Opt. Phys.* **39**, 4563 (2006).

¹² M. Krauss and W.J. Stevens, *J. Chem. Phys.* **93**, 4236 (1990).

¹³ J.Y. Seto, R.J. Le Roy, J. Vergès and C. Amiot, *J. Chem. Phys.* **113**, 3067 (2000)

¹⁴ C. Strauss, T. Takekoshi, F. Lang, K. Winkler, R. Grimm, J.H. Denschlag, and E. Tiemann, *Phys. Rev. A* **82**, 052514 (2010).

... information about most excited-state potentials is much thinner ...

- The mixing of the $A^1\Sigma_u^+$ and $b^3\Pi_u$ states has allowed them to be used as ‘doorways’ for accessing the triplet manifold, and an ambitious 4-state coupled-channel analysis has yielded analytic potentials that span much of their potential wells,¹⁵

¹⁵ A. Drozdova, A.V. Stolyarov, M. Tamanis, R. Ferber and A.J. Ross, *Phys. Rev. A* **88**, 022504 (2013).

... information about most excited-state potentials is much thinner ...

- The mixing of the $A^1\Sigma_u^+$ and $b^3\Pi_u$ states has allowed them to be used as ‘doorways’ for accessing the triplet manifold, and an ambitious 4-state coupled-channel analysis has yielded analytic potentials that span much of their potential wells,¹⁶ *however ...*

that analysis *did not* incorporate the known long-range inverse-power behaviour, that is *dominated most particularly* by the strong $1/r^3$ exchange-dipole term associated with states that dissociate to $nS + nP$ atomic thresholds.

¹⁶ A. Drozdova, A.V. Stolyarov, M. Tamanis, R. Ferber and A.J. Ross, *Phys. Rev. A* **88**, 022504 (2013).

... *information about most excited-state potentials is much thinner* ...

- The mixing of the $A^1\Sigma_u^+$ and $b^3\Pi_u$ states has allowed them to be used as ‘doorways’ for accessing the triplet manifold, and an ambitious 4-state coupled-channel analysis has yielded analytic potentials that span much of their potential wells,¹⁷ *however* ...

that analysis did not incorporate the known long-range inverse-power behaviour, that is *dominated most particularly* by the strong $1/r^3$ exchange-dipole term associated with states that dissociate to $nS + nP$ atomic thresholds.

- Double resonance spectroscopy has yielded extensive $^1\Pi_g$ state emission into the $B^1\Pi_u$ state which dissociates to the same $5S + 5P$ atomic threshold, and is predicted to have a repulsive barrier protruding above its asymptote,¹⁸

¹⁷ A. Drozdova, A.V. Stolyarov, M. Tamanis, R. Ferber and A.J. Ross, *Phys. Rev. A* **88**, 022504 (2013).

¹⁸ C. Amiot and J. Vergés, *Chem. Phys. Lett.* **274**,91 (1997).

... information about most excited-state potentials is much thinner ...

- The mixing of the $A^1\Sigma_u^+$ and $b^3\Pi_u$ states has allowed them to be used as ‘doorways’ for accessing the triplet manifold, and an ambitious 4-state coupled-channel analysis has yielded analytic potentials that span much of their potential wells,¹⁹ *however ...*

that analysis did not incorporate the known long-range inverse-power behaviour, that is *dominated most particularly* by the strong $1/r^3$ exchange-dipole term associated with states that dissociate to $nS + nP$ atomic thresholds.

- Double resonance spectroscopy has yielded extensive $^1\Pi_g$ state emission into the $B^1\Pi_u$ state which dissociates to the same $5S + 5P$ atomic threshold, and is predicted to have a repulsive barrier protruding above its asymptote,²⁰

however ...

The associated analysis involved only a classical Dunham expansion fit that allows one to perform a semiclassical “RKR” inversion to obtain turning points almost up to the top of the inner wall of the barrier, yet *neglected the long-range behaviour which gave rise to that barrier!*

¹⁹ A. Drozdova, A.V. Stolýarov, M. Tamanis, R. Ferber and A.J. Ross, *Phys. Rev. A* **88**, 022504 (2013).

²⁰ C. Amiot and J. Vergés, *Chem. Phys. Lett.* **274**,91 (1997).

... *information about most excited-state potentials is much thinner* ...

- The mixing of the $A^1\Sigma_u^+$ and $b^3\Pi_u$ states has allowed them to be used as ‘doorways’ for accessing the triplet manifold, and an ambitious 4-state coupled-channel analysis has yielded analytic potentials that span much of their potential wells,²¹ *however* ...

that analysis did not incorporate the known long-range inverse-power behaviour, that is *dominated most particularly* by the strong $1/r^3$ exchange-dipole term associated with states that dissociate to $nS + nP$ atomic thresholds.

- Double resonance spectroscopy has yielded extensive $^1\Pi_g$ state emission into the $B^1\Pi_u$ state which dissociates to the same $5S + 5P$ atomic threshold, and is predicted to have a repulsive barrier protruding above its asymptote,²²

however ...

- The associated analysis involved only a classical Dunham expansion fit which allows one to perform a semiclassical “RKR” inversion to obtain turning points up to near the top of the inner wall of the barrier and *neglected the long-range behaviour which gave rise to that barrier!*

- ***the present work intends to supplant that analysis!***

²¹ A. Drozdova, A.V. Stolýarov, M. Tamanis, R. Ferber and A.J. Ross, *Phys. Rev. A* **88**, 022504 (2013).

²² C. Amiot and J. Vergés, *Chem. Phys. Lett.* **274**,91 (1997).

Objectives of the present work

- To use a Direct Potential Fit (DPF) analysis of all available data to determine a global, fully analytic potential energy function for the $B^1\Pi_u$ “barrier” state of Rb_2

Objectives of the present work

- To use a Direct Potential Fit (DPF) analysis of all available data to determine a global, fully analytic potential energy function for the $B^1\Pi_u$ “barrier” state of Rb_2
- Since the data for the $B^1\Pi_u$ state consists mostly of transitions involving the $X^1\Sigma_g^+$ and/or $2^1\Pi_g$ state, our DPF analysis will simultaneously attempt also to determine (improved) global analytic potential functions for the (non-barrier) states.

Objectives of the present work

- To use a Direct Potential Fit (DPF) analysis of all available data to determine a global, fully analytic potential energy function for the $B^1\Pi_u$ “barrier” state of Rb_2
- Since the data for the $B^1\Pi_u$ state consists mostly of transitions involving the $X^1\Sigma_g^+$ and/or $2^1\Pi_g$ state, our DPF analysis will simultaneously attempt also to determine (improved) global analytic potential functions for the (non-barrier) states.
- We shall examine the effect of incorporating the interstate-coupling, known to be increasingly important near alkali dimer $nS + nP$ asymptotes, on the nature of the empirically-determined outer wall of the $B^1\Pi_u$ state potential.

Objectives of the present work

- To use a Direct Potential Fit (DPF) analysis of all available data to determine a global, fully analytic potential energy function for the $B^1\Pi_u$ “barrier” state of Rb_2
- Since the data for the $B^1\Pi_u$ state consists mostly of transitions involving the $X^1\Sigma_g^+$ and/or $2^1\Pi_g$ state, our DPF analysis will simultaneously attempt also to determine (improved) global analytic potential functions for the (non-barrier) states.
- We shall examine the effect of incorporating the interstate-coupling, known to be increasingly important near alkali dimer $nS + nP$ asymptotes, on the nature of the empirically-determined outer wall of the $B^1\Pi_u$ state potential.
- We shall test the efficacy of the new modified version of the “DELR” model used for the $B^1\Pi_u$ “barrier-state” potential of Li_2 .²³

²³ Y. Huang and R.J. Le Roy, *J. Chem. Phys.* **119**, 7398 (2003).

Methodology:

Direct Potential Fits consist of the following steps:

- assume an analytic functional form for the potential energy function of every electronic state involved in the spectra,
- obtain/generate/estimate plausible initial estimates for the parameters defining each of the relevant potentials,
- for the upper and lower level of every spectral transition, solve the radial Schrödinger equation to determine its eigenvalue $E_{v,J}$ to an accuracy an order of magnitude higher than the precision of the data associated with that level,
- employ the radial wavefunctions $\psi_{v,J}(r)$ obtained when solving for each of the vibration/rotational levels to calculate the exact partial derivatives of its eigenvalue with respect to all parameters p_k defining the potential energy function for that state:
$$\frac{\partial E_{v,J}}{\partial p_k} = \left\langle \psi_{v,J}(r) \left| \frac{\partial V(\{p_j\}; r)}{\partial p_k} \right| \psi_{v,J}(r) \right\rangle$$
- Use the partial derivatives in a ‘standard’ non-linear least-squares-fit program to optimize the values of all potential function parameters.

Tools:

- Program **betaFIT**²⁴ generates initial trial potential function expansion parameters from a set of RKR or *ab initio* turning points
- Program **dPotFit**²⁵ generates the synthetic spectra and performs least-squares fits to parameterized potential energy functions.

Functional Form for regular Single-Minimum Potentials

The *Morse/Long-Range (MLR) Potential*.

$$V_{\text{MLR}}(r) = \mathfrak{D}_e \left\{ 1 - \frac{u_{\text{LR}}(r)}{u_{\text{LR}}(r_e)} e^{-\beta(r) y_p^{\text{eq}}(r)} \right\}^2$$
$$\xrightarrow{r \gg r_e} \mathfrak{D}_e - \left[\frac{2\mathfrak{D}_e e^{-\beta\infty}}{u_{\text{LR}}(r_e)} \right] u_{\text{LR}}(r) = \mathfrak{D}_e - \frac{C_{m_1}}{r^{m_1}} - \frac{C_{m_2}}{r^{m_2}} - \dots$$

in which

$$u_{\text{LR}}(r) \equiv \sum_{i=1}^{\text{last}} D_{m_i}(r) \frac{C_{m_i}}{r^{m_i}} \simeq \frac{C_{m_1}}{r^{m_1}} + \frac{C_{m_2}}{r^{m_2}} + \dots$$

where $D_{m_i}(r)$ are ‘damping functions’ that approach 1 as $r \rightarrow \infty$,

and $\beta(r) = y_p(r) \beta_\infty + [1 - y_p(r)] \sum_j \beta_j \{y_q(r)\}^j$, with $y_q(r) \equiv \frac{r^q - (r_{\text{ref}})^q}{r^q + (r_{\text{ref}})^q}$.

²⁴see <http://leroy.uwaterloo.ca/programs/>

²⁵see <http://leroy.uwaterloo.ca/programs/>

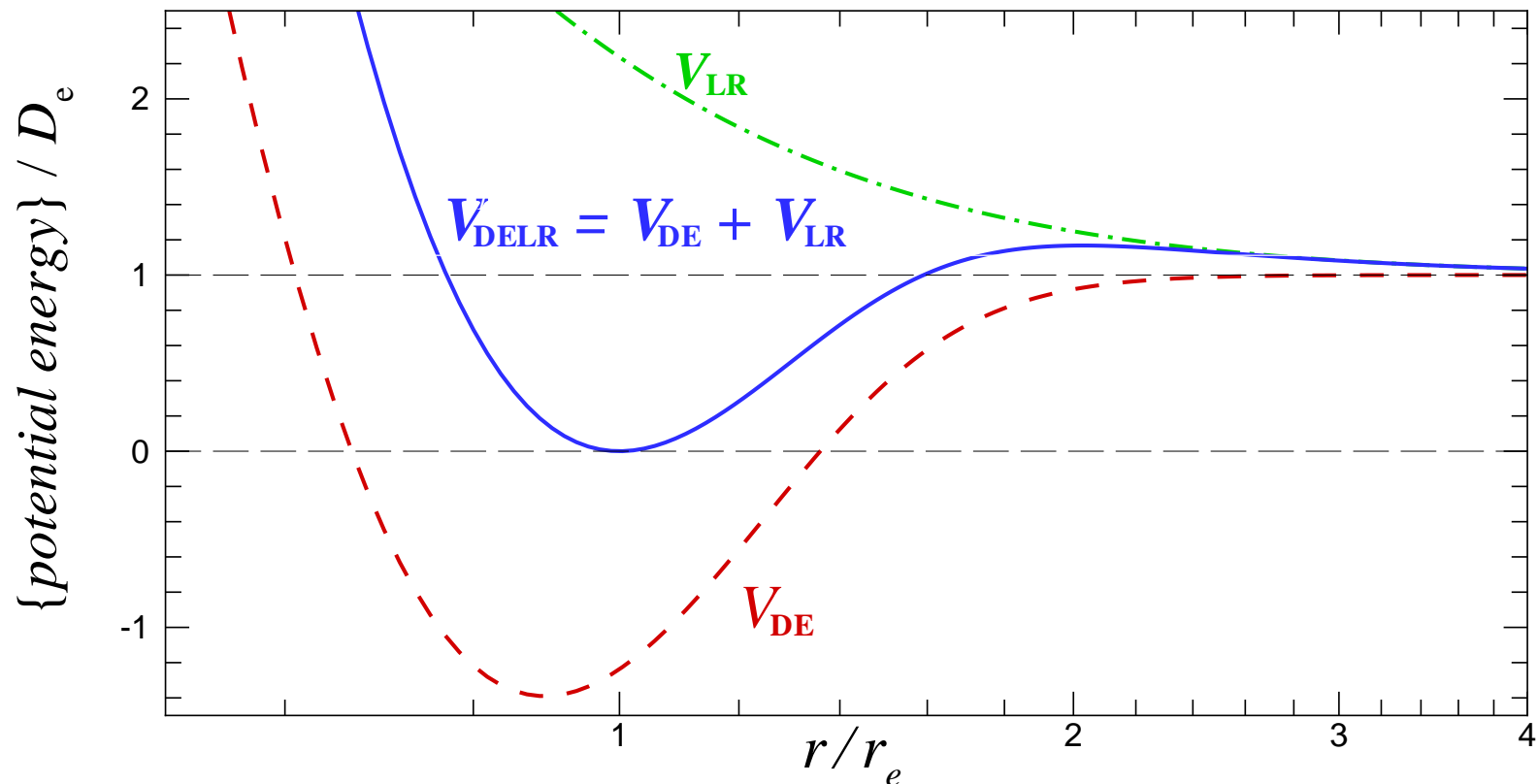
Functional Form for “barrier” Potentials

The Double-Exponential/Long-Range (DELR) Potential.

$$V_{\text{DELR}}(r) = \left[A e^{-2\beta(y_q)(r-r_e)} - B e^{-2\beta(y_q)(r-r_e)} + \mathcal{D}_e \right] - u_{\text{LR}}(r)$$
$$\xrightarrow{r \gg r_e} \mathcal{D}_e - u_{\text{LR}}(r) \simeq \mathcal{D}_e - \frac{C_{m_1}}{r^{m_1}} - \frac{C_{m_2}}{r^{m_2}} - \dots$$

with $A = \mathcal{D}_e - u_{\text{LR}}(r_e) + u'_{\text{LR}}(r_e)/\beta(r_e)$

and $B = \mathcal{D}_e - 2u_{\text{LR}}(r_e) + u'_{\text{LR}}(r_e)/\beta(r_e)$



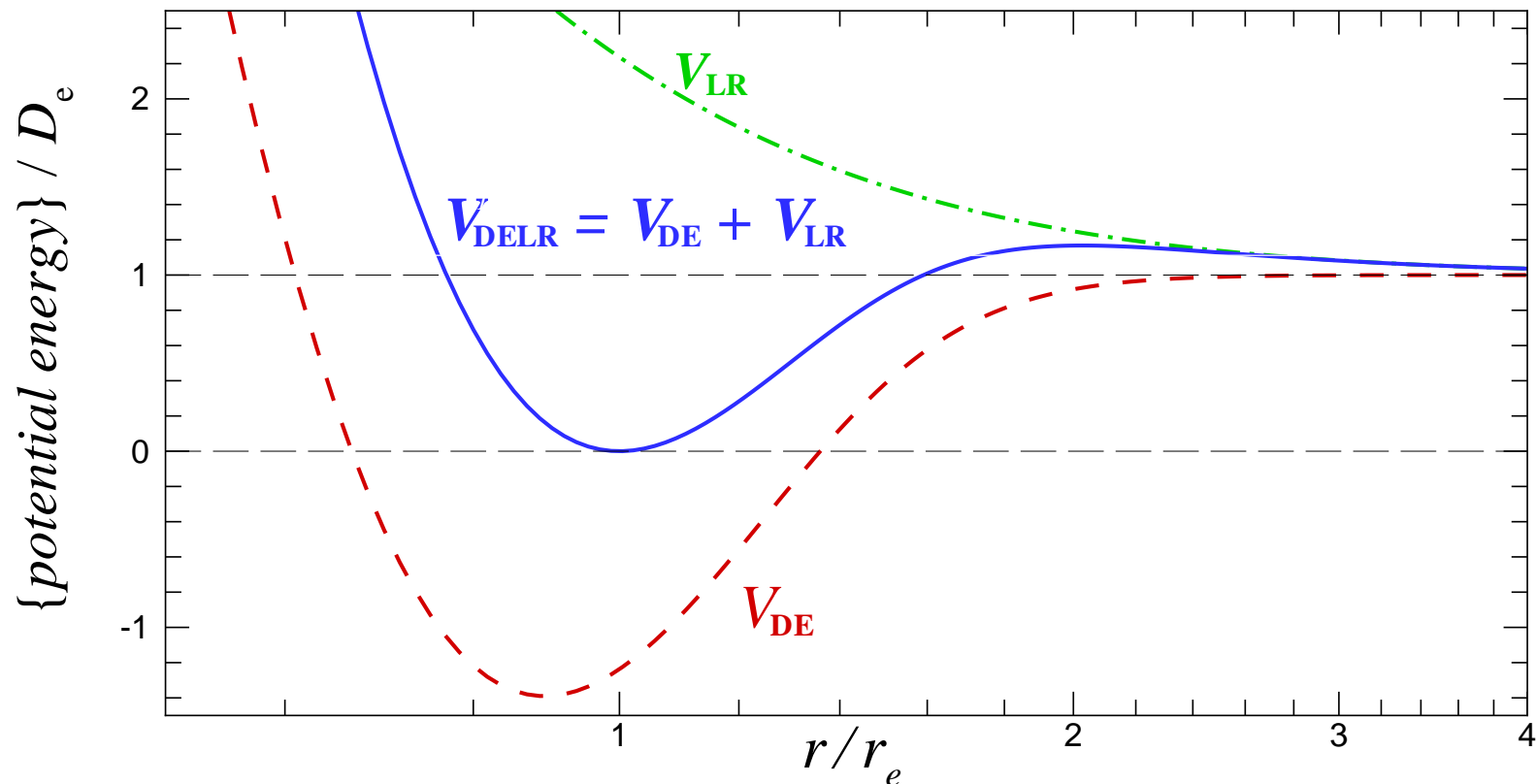
Functional Form for “barrier” Potentials

The Double-Exponential/Long-Range (DELR) Potential.

$$V_{\text{DELR}}(r) = \left[A e^{-2\beta(y_q)(r-r_e)} - B e^{-2\beta(y_q)(r-r_e)} + \mathcal{D}_e \right] - u_{\text{LR}}(r)$$
$$\xrightarrow{r \gg r_e} \mathcal{D}_e - u_{\text{LR}}(r) \simeq \mathcal{D}_e - \frac{C_{m_1}}{r^{m_1}} - \frac{C_{m_2}}{r^{m_2}} - \dots$$

with $A = \mathcal{D}_e - u_{\text{LR}}(r_e) + u'_{\text{LR}}(r_e)/\beta(r_e)$

and $B = \mathcal{D}_e - 2u_{\text{LR}}(r_e) + u'_{\text{LR}}(r_e)/\beta(r_e)$



... but how should we represent the long-range barrier-wall function $u_{\text{LR}}(r)$?

... how should we represent the long-range barrier-wall function $u_{\text{LR}}(r)$?

In our previous study of the analogous $B^1\Pi_u$ state of Li_2 ,²⁶ the repulsive long-range part of the DELR potential was represented by a conventional sum of damped inverse-power term ...

$$u_{\text{LR}}(r) \equiv \sum_{i=1}^{\text{last}} D_{m_i}(r) \frac{C_{m_i}}{r^{m_i}} \simeq \frac{C_{m_1}}{r^{m_1}} + \frac{C_{m_2}}{r^{m_2}} + \dots$$

²⁶ Y. Huang and R.J. Le Roy, *J. Chem. Phys.* **119**,7398 (2003).

... how should we represent the long-range barrier-wall function $u_{\text{LR}}(r)$?

In our previous study of the analogous $B^1\Pi_u$ state of Li_2 ,²⁷ the repulsive long-range part of the DELR potential was represented by a conventional sum of damped inverse-power term ...

$$u_{\text{LR}}(r) \equiv \sum_{i=1}^{\text{last}} D_{m_i}(r) \frac{C_{m_i}}{r^{m_i}} \simeq \frac{C_{m_1}}{r^{m_1}} + \frac{C_{m_2}}{r^{m_2}} + \dots$$

However, theory tells us that it should be represented by the middle eigenvalue of the 3×3 matrix $\mathbf{M}_{\text{LR}}(r)$:²⁸

$$- \begin{pmatrix} \sum_{n=3,6,8\dots} D_n(r) \frac{C_n^{3\Sigma} + C_n^{1\Pi} + C_n^{3\Pi}}{3r^n} & \sum_{n=3,6,8\dots} D_n(r) \frac{C_n^{3\Pi} + C_n^{1\Pi} - 2C_n^{3\Sigma}}{3\sqrt{2}r^n} & \sum_{n=3,6,8\dots} D_n(r) \frac{C_n^{3\Pi} - C_n^{1\Pi}}{\sqrt{6}r^n} \\ \sum_{n=3,6,8\dots} D_n(r) \frac{C_n^{3\Pi} + C_n^{1\Pi} - 2C_n^{3\Sigma}}{3\sqrt{2}r^n} & \sum_{n=3,6,8\dots} D_n(r) \frac{C_n^{3\Pi} + C_n^{1\Pi} + 4C_n^{3\Sigma}}{6r^n} + V_{\text{LIM}} & \sum_{n=3,6,8\dots} D_n(r) \frac{C_n^{3\Pi} - C_n^{1\Pi}}{2\sqrt{3}r^n} \\ \sum_{n=3,6,8\dots} D_n(r) \frac{C_n^{3\Pi} - C_n^{1\Pi}}{\sqrt{6}r^n} & \sum_{n=3,6,8\dots} D_n(r) \frac{C_n^{3\Pi} - C_n^{1\Pi}}{2\sqrt{3}r^n} & \sum_{n=3,6,8\dots} D_n(r) \frac{C_n^{3\Pi} + C_n^{1\Pi}}{2r^n} + V_{\text{LIM}} \end{pmatrix}$$

The present work will compare these two models and determine whether the experimental data can distinguish between them!

²⁷ Y. Huang and R.J. Le Roy, *J. Chem. Phys.* **119**, 7398 (2003).

²⁸ M. Aubert-Frécon, G. Hadinger, S. Magnier and S. Rousseau, *J. Mol. Spectrosc.* **188**, 182 (1998).

Results: ... and with 44 fitting parameters get $\overline{dd} = 1.63$ (over 30,169 data).

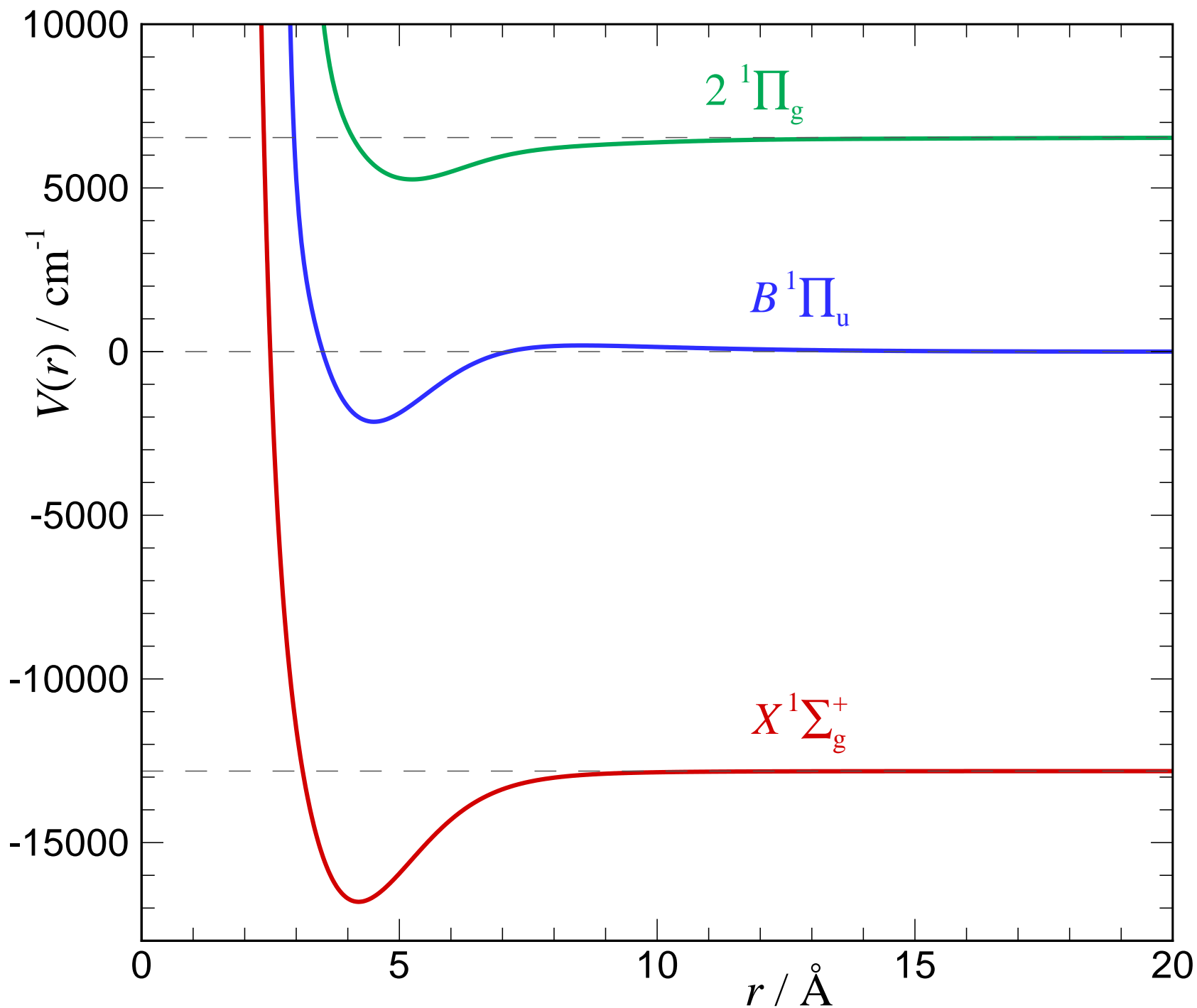
	$X^1\Sigma_g^+$ (MLR)	$B^1\Pi_u$ (DELR)	$2^1\Pi_g$ (MLR)
V_{LIM}	[-12816.545]	[0]	[6539.0665]
\mathcal{D}_e	3993.618 (13)	2144.68842 (920)	1279.6087 (93)
r_e	4.209929 (41)	4.506241 (26)	5.246006 (38)
C_3^Σ	—	$[-5.984 \times 10^5]$	—
$C_3^1\Pi$	—	$[-2.992 \times 10^5]$	—
$C_3^3\Pi$	—	$[2.992 \times 10^5]$	—
C_5	—	—	$[8.894 \times 10^6]$
C_6^Σ	$[2.2338 \times 10^7]$	$[5.807 \times 10^7]$	—
$C_6^1\Pi$	—	$[3.878 \times 10^7]$	$[7.1375 \times 10^7]$
$C_6^3\Pi$	—	$[3.878 \times 10^7]$	—
C_8^Σ	$[7.6939 \times 10^8]$	$[1.277 \times 10^{10}]$	—
$C_8^1\Pi$	—	$[1.528 \times 10^9]$	$[2.4584 \times 10^9]$
$C_8^3\Pi$	—	$[5.672 \times 10^8]$	—
C_{10}	$[2.9916 \times 10^{10}]$	—	—
$\{p, q\}$	{5, 3}	{-, 3}	{5, 3}
r_{ref}	[5.73]	[4.7]	[7.6]
β_0	0.0898006	0.7410021	0.616469
β_1	-0.74343386	0.283468	1.04582
β_2	-0.3428	0.163047	-1.617
β_3	0.67605	0.19056	-5.6496
β_4	1.1796093	0.1666	2.646
β_5	1.2845	0.148	2..41
β_6	1.3819	-1.5254	-8.
β_7	1.994	-0.689	-96.70655
β_8	1.495	4.641	-57.9
β_9	-0.7	-3.67	181.6
β_{10}	-2.	—	284.772
β_{10}	-2.28	—	120.
β_{11}	-4.1068	—	—
β_{12}	-3.55	—	—
β_{13}	-3.994	—	—
$\{p_{\text{ad}}, q_{\text{ad}}\}$	{n/a}	{3, 3}	{3, 3}
u_0	—	-0.123(69)	0.20(7)
u_1	—	-1.03	-23.7
u_2	—	—	30.
u_3	—	—	20.
u_∞	—	[0.0]	[0.0]

Results: Compare fitted parameters of our MLR model for the $X^1\Sigma_g^+$ state with those defining the ‘Hannover Polynomial Potential’ (HPP) model of Strauss *et al.*²⁹

	MLR(present)		HPP(Strauss)
\mathcal{D}_e	3993.618 (12)		3993.593 (3)
r_e	4.209929 (4)		3.02991 (5)
β_0	0.0898006	a_0	3.993592873×10^3
β_1	-0.74343386	a_1	0.000000000000000000
β_2	-0.3428	a_2	$0.282069372972346137 \times 10^5$
β_3	0.67605	a_3	$0.560425000209256905 \times 10^4$
β_4	1.1796093	a_4	$-0.423962138510562945 \times 10^5$
β_5	1.2845	a_5	$-0.598558066508841584 \times 10^5$
β_6	1.3819	a_6	$-0.162613532034769596 \times 10^5$
β_7	1.994	a_7	$-0.405142102246254944 \times 10^5$
β_8	1.495	a_8	$0.195237415352729586 \times 10^6$
β_9	-0.7	a_8	$0.413823663033582852 \times 10^6$
β_{10}	-2.	a_{10}	$-0.425543284828921501 \times 10^7$
β_{10}	-2.28	a_{11}	$0.546674790157210198 \times 10^6$
β_{11}	-4.1068	a_{12}	$0.663194778861331940 \times 10^8$
β_{12}	-3.55	a_{13}	$-0.558341849704095051 \times 10^8$
β_{13}	-3.994	a_{14}	$-0.573987344918535471 \times 10^9$
		a_{15}	$0.102010964189156187 \times 10^{10}$
		a_{16}	$0.300040150506311035 \times 10^{10}$
		a_{17}	$-0.893187252759830856 \times 10^{10}$
		a_{18}	$-0.736002541483347511 \times 10^{10}$
		a_{19}	$0.423130460980355225 \times 10^{11}$
		a_{20}	$-0.786351477693491840 \times 10^{10}$
		a_{21}	$-0.102470557344862152 \times 10^{12}$
		a_{22}	$0.895155811349267578 \times 10^{11}$
		a_{23}	$0.830355322355692902 \times 10^{11}$
		a_{24}	$-0.150102297761234375 \times 10^{12}$
		a_{25}	$0.586778574293387070 \times 10^{11}$

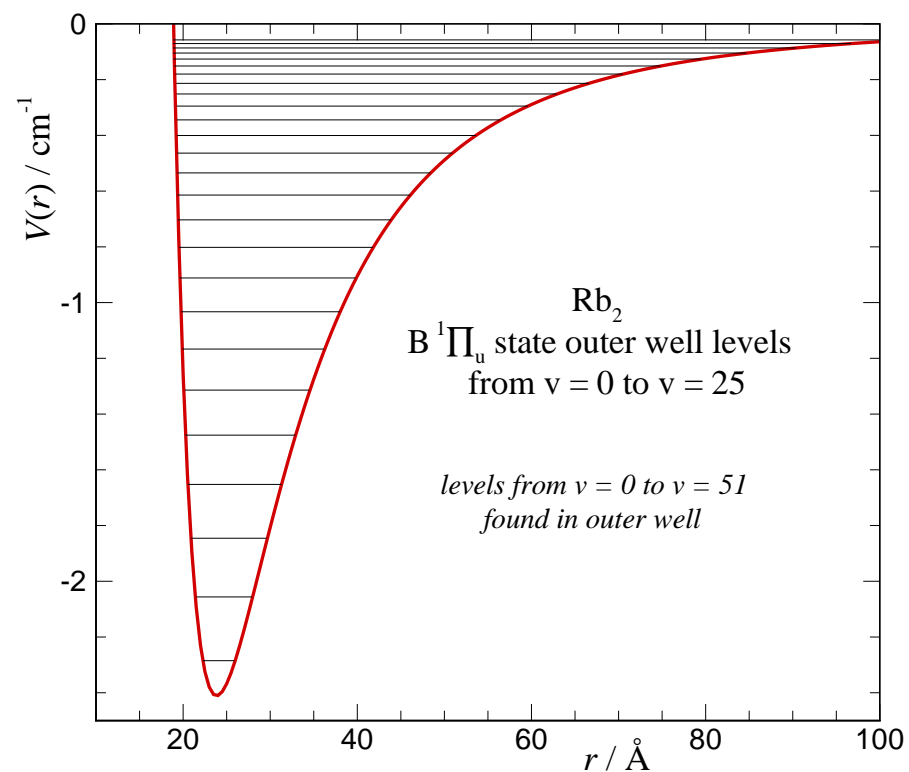
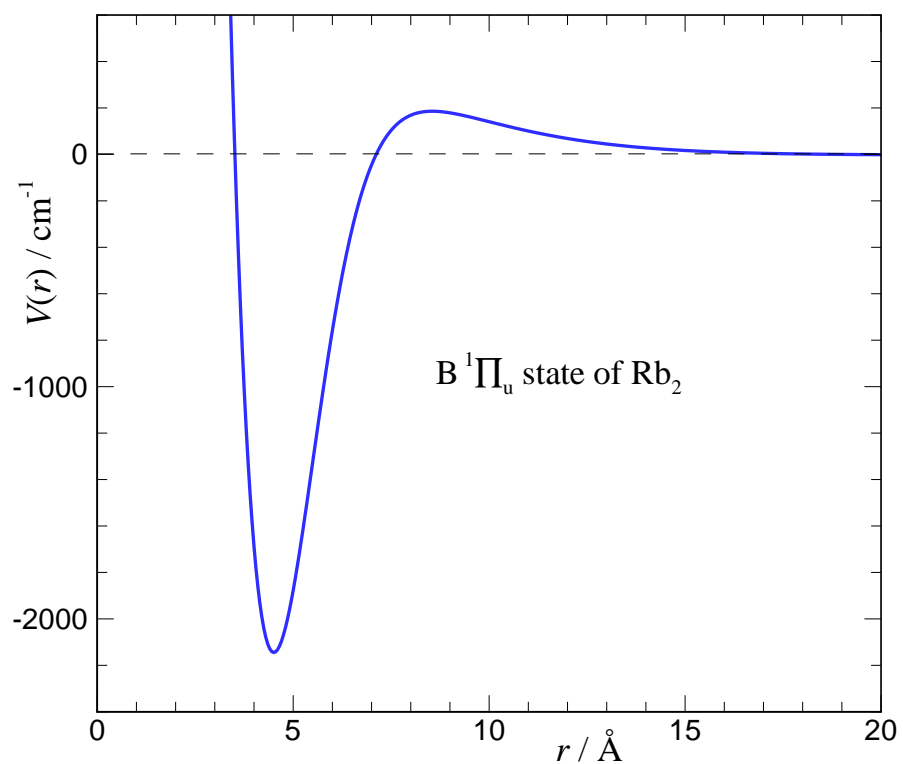
²⁹ C. Strauss, T. Takekoshi, F. Lang, K. Winkler, R. Grimm, J.H. Denschlag, and E. Tiemann, *Phys. Rev. A* **82**, 052514 (2010).

Results: Our analysis yields accurate analytic potentials for the three states!



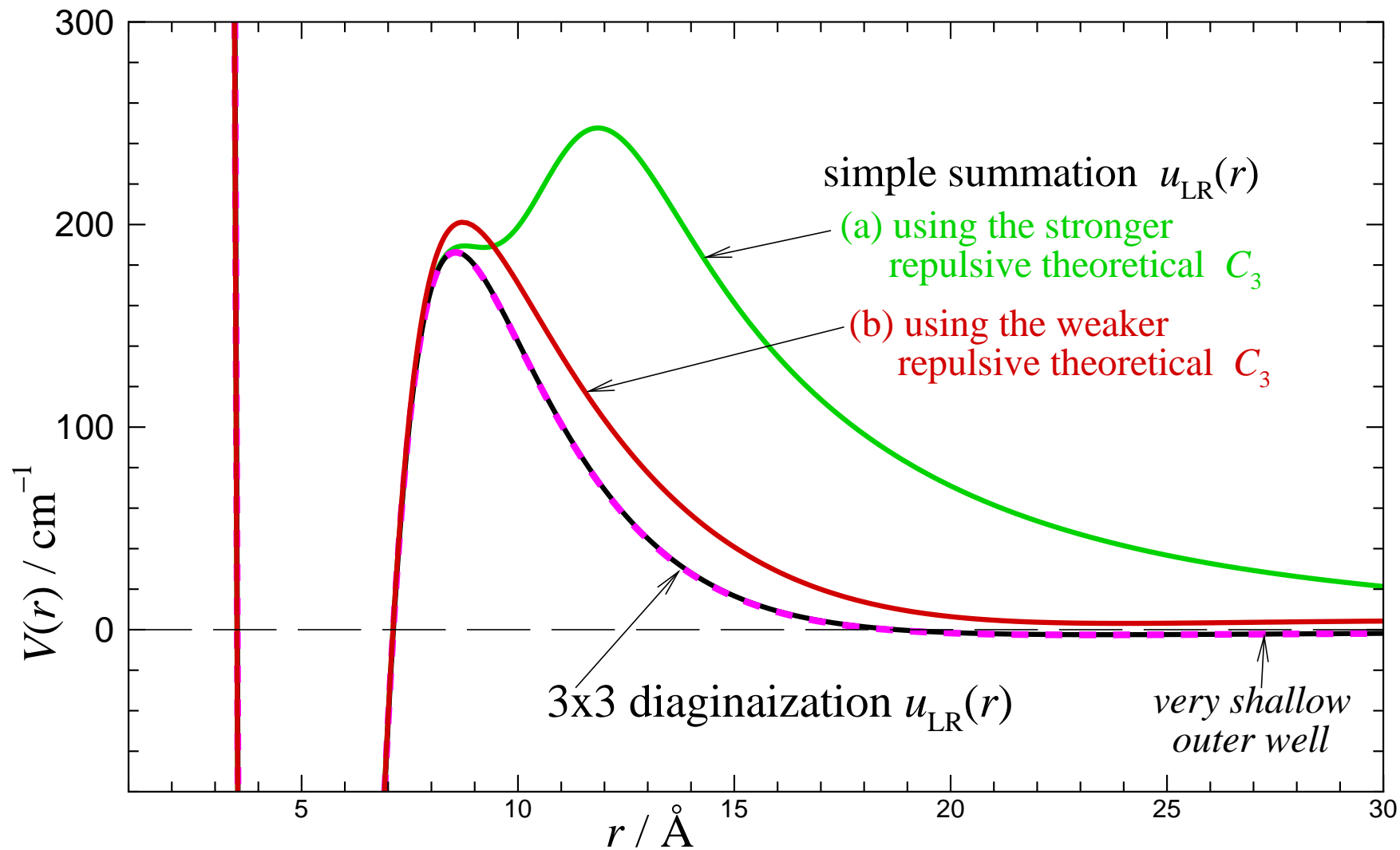
Results:

... and in addition to determining the $B^1\Pi_u$ state potential well and barrier properties, the present analysis delineates the properties of its long-predicted³⁰ outer well centred at 24 Å, which is found to support 51 vibrational levels!



³⁰ M. Movre and G. Pichler, *J. Phys. B: At. Mol. Phys.* **10**, 2631 (1977).

Results: { Conclusions re. for 3×3 vs. simple sum, for $u_{\text{LR}}(r)$ not yet fully clear ... ! }



Conclusions:

- We have determined fully analytic PECs for the $X^1\Sigma_g^+$, $B^1\Pi_u$, and $2^1\Pi_g$ states of Rb_2 whose *44 fitted parameters* compactly summarize our spectroscopic knowledge of these species.

In particular, they describe all **30,169** accessible data for these states (on average) within their ($0.02 - 0.001 \text{ cm}^{-1}$) uncertainties.

Conclusions:

- We have determined fully analytic PECs for the $X^1\Sigma_g^+$, $B^1\Pi_u$, and $2^1\Pi_g$ states of Rb_2 whose *44 fitted parameters* compactly summarize our spectroscopic knowledge of these species.

In particular, they describe all *30,169* accessible data for these states (on average) within their (*0.02 – 0.001 cm⁻¹*) uncertainties.

- This work shows that our DELR potential function model can readily incorporate representing the repulsive term giving rise to the $B^1\Pi_u$ -state barrier by the middle eigenvalue of the 3×3 “Aubert-Frecon” long-range interaction matrix for $nS + nP$ alkali dimers,

Conclusions:

- We have determined fully analytic PECs for the $X^1\Sigma_g^+$, $B^1\Pi_u$, and $2^1\Pi_g$ states of Rb_2 whose *44 fitted parameters* compactly summarize our spectroscopic knowledge of these species.

In particular, they describe all *30,169* accessible data for these states (on average) within their (*0.02 – 0.001 cm⁻¹*) uncertainties.

- This work shows that our DELR potential function model can readily incorporate representing the repulsive term giving rise to the $B^1\Pi_u$ -state barrier by the middle eigenvalue of the 3×3 “Aubert-Frecon” long-range interaction matrix for $nS + nP$ alkali dimers,
- The isotopologue-dependence of the ground $X^1\Sigma_g^+$ -state well depth is too small to be determined from the available data, *... however ...*
the (small) electronic isotope shifts of the $B^1\Pi_u$, and $2^1\Pi_g$ states *are* clearly discerned.

Conclusions:

- We have determined fully analytic PECs for the $X^1\Sigma_g^+$, $B^1\Pi_u$, and $2^1\Pi_g$ states of Rb_2 whose *44 fitted parameters* compactly summarize our spectroscopic knowledge of these species.

In particular, they describe all *30,169* accessible data for these states (on average) within their (*0.02 – 0.001 cm⁻¹*) uncertainties.

- This work shows that our DELR potential function model can readily incorporate representing the repulsive term giving rise to the $B^1\Pi_u$ -state barrier by the middle eigenvalue of the 3×3 “Aubert-Frecon” long-range interaction matrix for $nS + nP$ alkali dimers,
- The isotopologue-dependence of the ground $X^1\Sigma_g^+$ -state well depth is too small to be determined from the available data, *... however ...*
the (small) electronic isotope shifts of the $B^1\Pi_u$, and $2^1\Pi_g$ states *are* clearly discerned.
- An isotopologue-dependent 3-parameter “effective non-adiabatic” centrifugal BOB function must be included in the model for the $B^1\Pi_u$ state to fully explain the data.